

Peer Reviewed Letter openaccess

# Data processing of three-dimensional vibrational spectroscopic chemical images for pharmaceutical applications

#### Hannah Carruthers, a.b Don Clark, Fiona C. Clarke, Karen Faulds and Duncan Grahama.\*

<sup>a</sup>University of Strathclyde, Department of Pure and Applied Chemistry, George Street, Glasgow, G1 1RD, UK

<sup>b</sup>Pfizer Ltd, Ramsgate Road, Sandwich, Kent CT19 9NJ, UK

#### Contacts

H. Carruthers: <a href="mailto:hannah.carruthers@strath.ac.uk">hannah.carruthers@strath.ac.uk</a></a>
<a href="mailto:https://orcid.org/0000-0003-1702-4351">https://orcid.org/0000-0003-1702-4351</a>

D. Clark: don.a.clark@pfizer.com F.C. Clarke: fiona.clarke@pfizer.com K. Faulds: karen.faulds@strath.ac.uk

https://orcid.org/0000-0002-5567-7399

D. Graham: duncan.graham@strath.ac.uk

6 https://orcid.org/0000-0002-6079-2105

Vibrational spectroscopic chemical imaging is a powerful tool in the pharmaceutical industry to assess the spatial distribution of components within pharmaceutical samples. Recently, the combination of vibrational spectroscopic chemical mapping with serial sectioning has provided a means to visualise the three-dimensional (3D) structure of a tablet matrix. There are recognised knowledge gaps in current tablet manufacturing processes, particularly regarding the size, shape and distribution of components within the final drug product. The performance of pharmaceutical tablets is known to be primarily influenced by the physical and chemical properties of the formulation. Here, we describe the data processing methods required to extract quantitative domain size and spatial distribution statistics from 3D vibrational spectroscopic chemical images. This provides a means to quantitatively describe the microstructure of a tablet matrix and is a powerful tool to overcome knowledge gaps in current tablet manufacturing processes, optimising formulation development.

Keywords: 3D imaging, Raman, near infrared, infrared, chemical imaging, FIJI, ImageJ, image processing, image analysis, 3D

# Introduction

The performance of pharmaceutical tablets is primarily influenced by the physical and chemical properties of the formulation. The size and spatial arrangement of the active pharmaceutical ingredient (API) within the excipient matrix can influence the bioavailability, dissolution rate and stability of the final drug product.<sup>1-4</sup> Vibrational spectroscopic chemical mapping is an established tool

within the pharmaceutical industry to examine the size and spatial arrangement of components within tablets.<sup>5-9</sup> Traditional applications usually involve only examining a single exposed surface area of a sample and thus there are known limitations associated with obtaining domain size statistics from a two-dimensional (2D) chemical image.<sup>10</sup> Recently, the combination of spectroscopic

#### Correspondence

Duncan Graham: duncan.graham@strath.ac.uk

Received: 18 March 2022 Revised: 28 March 2022 Accepted: 28 March 2022 Publication: 30 March 2022 doi: 10.1255/jsi.2022.a3 ISSN: 2040-4565

#### Citation

H. Carruthers, D. Clark, F.C. Clarke, K. Faulds and D. Graham, "Data processing of three-dimensional vibrational spectroscopic chemical images for pharmaceutical applications", *J. Spectral Imaging* **11**, a3 (2022). <a href="https://doi.org/10.1255/jsi.2022.a3">https://doi.org/10.1255/jsi.2022.a3</a>

© 2022 The Authors

This licence permits you to use, share, copy and redistribute the paper in any medium or any format provided that a full citation to the original paper in this journal is given.



mapping with serial sectioning has enabled full visualisation of the three-dimensional (3D) microstructure of a tablet system to be achieved. A 3D dataset can be reconstructed by stacking individual 2D chemical images collected at regular depth intervals into the sample. To further enhance the added value of 3D spectroscopic mapping methods, this paper outlines the methods required to visualise, process and analyse 3D volumetric data for pharmaceutical applications.

Particle size is a crucial parameter in pharmaceutical manufacturing processes and is tightly controlled to ensure product quality.<sup>12</sup> The particle size distribution (PSD) of the API and excipients can significantly affect the efficacy (dissolution rate, bioavailability, uniformity and stability) and safety (content uniformity) of the final drug product. 13,14 There are a range of established techniques available to characterise the particle size of the raw API and excipient material (laser diffraction, dynamic light scattering, microscopy/image analysis),15 however, this does not always reflect the true size of the component domains once compacted into a tablet. Tablet manufacturing consists of a number of processing steps (including mixing, granulating, drying, blending, compaction and coating) where the ingoing material undergoes physical (mechanical and thermal) stress.16 There are knowledge gaps in current tablet manufacturing processes regarding the PSD of the API and excipients within the final drug product.

The spatial arrangement of components within a tablet can also significantly influence drug product performance. <sup>17</sup> Successful tablet formation requires dominating bonding mechanisms between components. <sup>18</sup> A change in the spatial arrangement of components within the formulation can lead to alternative bonding mechanisms during

compaction which may affect the stability of the tablet. The location of the API relative to the excipient matrix may also influence the dissolution profile and bioavailability of the drug product. New methods to quantitatively describe the size and distribution of a component within a tablet matrix are required for improved tablet manufacturing and product performance understanding.

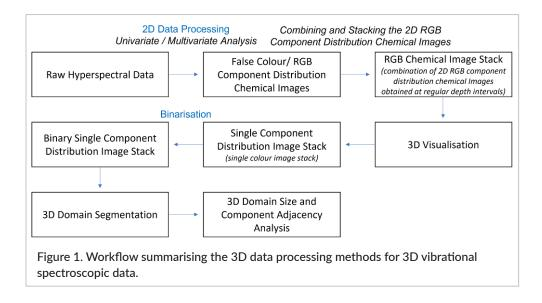
FIJI<sup>19</sup> (an extension of ImageJ<sup>20</sup>) is an open-source image processing software specifically designed for the analysis of multidimensional scientific images. There are numerous plugins and scripts available for a wide range of applications. Three-dimensional image processing capabilities have been extensively explored for biological<sup>19</sup> and biomedical<sup>21</sup> samples, however, there has been no literature documented for pharmaceutical 3D spatial distribution analysis. In this paper, we describe the methods required to process 3D spectroscopic data to visualise and quantify the size and spatial arrangement of components within pharmaceutical tablets.

## Methods

A workflow summarising the data processing methods for 3D vibrational spectroscopic chemical imaging for understanding the size and distribution of components within pharmaceutical samples is summarised in Figure 1.

# Data collection and hyperspectral data processing

A 3D image of a sample can be obtained by combining serial sectioning with vibrational spectroscopic chemical imaging. 2D chemical images can be obtained at



regular depth intervals into a sample by physically milling and examining the exposed surface. Each 2D chemical imaging dataset is represented by a 3D hyperspectral data cube where two axes describe the x- and y-spatial dimensions and the third dimension represents the spectral wavelength. Data processing is a crucial aspect of chemical imaging to extract useful information from the large amount of data that has been collected. Spectral pre-processing, including background subtraction and cosmic ray rejection, may be required to remove or correct spectral and spatial artefacts before further processing.<sup>22</sup> Univariate or multivariate analysis can then be used to generate red-green-blue (RGB) images displaying the spatial distribution of components for each hyperspectral data cube.<sup>23</sup>

#### 3D data reconstruction and visualisation

To generate a 3D dataset, the individual 2D RGB chemical images, representing the spatial distribution of components, acquired at regular depth intervals can be combined to form an image stack. Once combined to an image stack, each pixel in the original 2D chemical images transforms to a voxel (volumetric pixel) with a z-dimension equal to the depth interval between chemical maps. Here, the image stack is represented by a 4D data cube where three axes describe the x-, y- and z-spatial dimensions and the fourth dimension represents the component identity through a RGB colour plane.

The FIJI 3D Viewer plugin<sup>24</sup> can be used to visualise the image stack in 3D space. The data can be visualised as either a volume or an orthoslice. Volume visualisation displays the data as a volume, while orthoslices enables slices orthogonal to the XY plane to be assessed and extracted to examine domains within the core of the dataset. The image stack can also be manipulated to visualise the 3D distribution of each component independently or together.

Visualising the tablet matrix in 3D enables the size, shape and distribution of components to be qualitatively inspected to gain a greater understanding of the microstructure of the drug product. As the volume of data increases, it is progressively more challenging to objectively examine and understand the 3D structure of the sample. Quantitative methods are required to measure the size distribution of each component and their relative position within the tablet matrix. Obtaining numerical domain size and adjacency statistics enables the size and distribution of components to be objectively compared across datasets and samples.

#### 3D domain segmentation and size analysis

There are several plugins available in FIJI capable of performing 3D domain size statistics. 3D Object Counter<sup>25</sup> and DiAna<sup>26</sup> (distance analysis) were found to be the most suitable plugins for pharmaceutical applications. Both plugins follow the same basic principles which involve, first, performing 3D domain segmentation, followed by domain size quantification.

Segmentation (illustrated in Figure 2) is a crucial process in image analysis used to extract and isolate individual domains. Single component image stacks are required for segmentation and, thus, the RGB image stack must first be split into individual component channels. A suitable threshold is applied to the grey-scale single component image stack to produce a binarised image stack. All pixels with a value greater than the threshold value correspond to the component and are assigned with an intensity value of "1" (coloured white). All pixels below the threshold value are given an intensity value of O (coloured black) and are considered not belonging to the component. The segmentation process involves labelling pixels to a numbered domain (or background). Domains are located by performing a 2-pass connexity analysis, illustrated in Figure 2(b). The image stack is scanned from the top left-hand corner to the bottom right-hand corner. When a pixel with an intensity value of "1" is located, it is assigned with a label. All 26 neighbouring pixels in a 3×3×3-pixel cube, including pixels on adjacent chemical maps are checked for an existing label. If a neighbouring pixel has an existing label, the new pixel is assigned with the same label. This identifies both pixels as belonging to the same domain. The second pass ensures all adjacent pixels are assigned with the same label, for example a "U" shaped domain connected by only its bottom parts may have been labelled separately in the first pass, however, can be identified as a single domain in the second pass. The output quantifies the number of domains of each component and produces a 3D representation of their location within the dataset.

The size and shape of each domain can be assessed by calculating its volume and surface area from the voxel pixels. A volumetric domain size distribution can be determined for each component to provide enhanced understanding of the size distribution of domains within the tablet matrix. Combining volume and surface area information can provide an improved understanding of the shape distribution of domains within the sample. These tools will be specifically valuable to quantify subtle differences in the size and shape of components across different samples which cannot be easily determined from

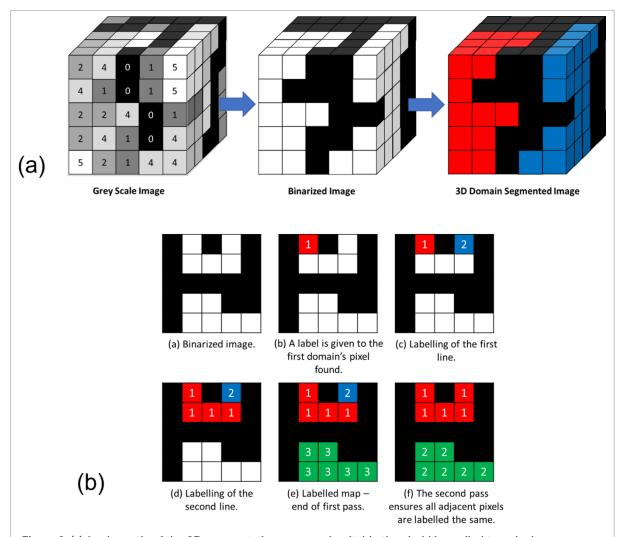


Figure 2. (a) A schematic of the 3D segmentation process. A suitable threshold is applied to a single component grey-scale image stack to produce a binarised image stack. The binarised image stack then undergoes a 2-pass connexity analysis to identify, label and locate all domains within 3D space (all neighbouring pixels with an intensity value of "1" are grouped as a single domain). (b) A schematic representation of the 2-pass connexity analysis process. Figure adapted from Bolte and Cordelières.<sup>25</sup>

visual inspection. Examples include understanding how the size and shape of domains change under different processing conditions or understanding out-of-specification (OOS) batches.

#### 3D component adjacency analysis

The spatial arrangement of components within a tablet matrix can be quantified by determining 3D component adjacencies statistics. The surface area (SA) in contact between domains of two components can be calculated to provide superior knowledge on the position of a component within a drug matrix relative to the other materials.

The SA in contact method for determining domain adjacency between two components is illustrated and

summarised in Figure 3. The basic principle of the method involves determining the total SA in contact between two components by calculating the total SA of the domains of each component both independently and combined. A combined image stack of the two components of interest can be generated by the addition of the individual single component image stacks using FIJI's "Image Calculator" command. Binarising the combined image stack eliminates the distinction between pixels corresponding to each component and thus 3D segmentation will group neighbouring pixels irrespective of their component identity. The 3D domain size plugins discussed earlier (3D Object Counter<sup>25</sup> and DiAna<sup>26</sup>) can be used to determine the total SA of all domains for the single component

image stacks and the combined image stack. The SA in contact between the two components can then be calculated using Equation (1).

 $\Sigma$  Contact SA(1,2) =

 $\underline{\left(\Sigma \text{SA1} \, domains + \Sigma \text{SA2} \, domains\right) - \Sigma \text{SA} \, combined 1, 2 \, domains}$ 

where:

 $\Sigma$ Contact SA(1,2) = Total SA in contact between component 1 and 2 domains

 $\Sigma$ SA 1 domains = Total SA of Component 1 domains  $\Sigma$ SA 2 domains = Total SA of Component 2 domains  $\Sigma$ SA combined 1,2 domains = Total SA of domains in combined Component 1+2 image stack

The SA in contact between two components can be expressed as a percentage SA of one component in contact with a second component. For example, the percentage surface area of API domains adjacent to the major excipient. This process can be repeated for all possible two-component combinations in the formulation to understand the relative spatial arrangement of all components within the tablet matrix. The sum of the percentage SA of a component in contact with all other components in the formulation may not equal 100% due to the presence of domains at the edge of the dataset and, thus, their domain adjacencies are unknown. The total SA not accounted for in the calculation will correspond to the surface area of the

whole dataset. This method provides superior knowledge on the relative position of a component within a drug matrix and can be used to quantitatively compare differences in the spatial arrangement of components across samples.

#### Case study

(1)

This case study showcases the data processing methods discussed above using a real Raman dataset that we published in the *Journal of Raman Spectroscopy*. <sup>11</sup> The 3D data processing workflow is documented in Figure 4.

The dataset comprised of 26 Raman chemical maps  $[500\,\mu\text{m}~(x)\times500\,\mu\text{m}~(y),~20\,\mu\text{m}~XY$  spatial step size] obtained at  $20\,\mu\text{m}$  depth intervals into the sample, resulting in a 3D dataset with the dimensions of  $500\,\mu\text{m}~(x)\times500\,\mu\text{m}~(y)\times520\,\mu\text{m}~(z)$ . The sample analysed was a model tablet containing three components: one active pharmaceutical ingredient (red) and two excipients (blue and green).

The RGB Raman maps showing the distribution of the three components were imported into FIJI as an image stack. The loaded image stack was then calibrated to ensure the pixel size and voxel depth were consistent with the experimental parameters. The image stack was then visualised using the 3D Viewer<sup>24</sup> plugin as both a 3D volume and an orthoslice. To objectively assess the 3D microstructure of the tablet system, the image stack was then separated into its individual single colour (component) image stacks to perform domain size and

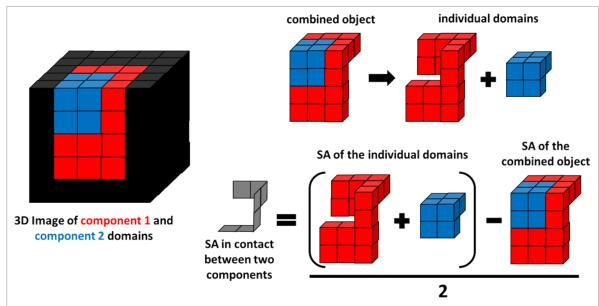
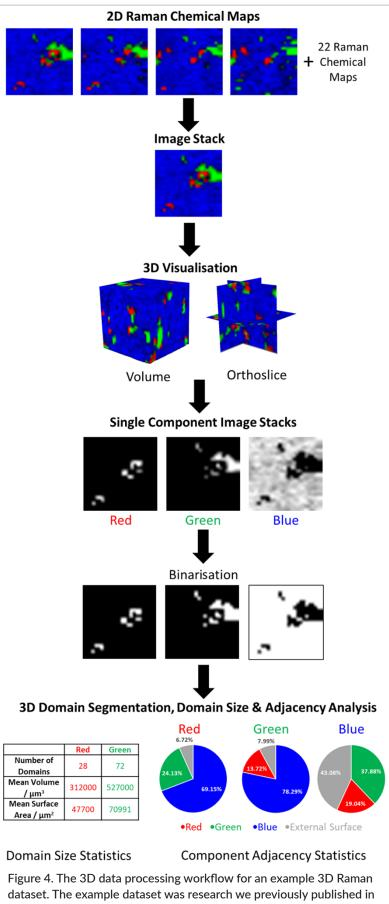


Figure 3. A schematic of the 3D domain adjacency process. The SA in contact between domains of two components is calculated by determining the SA of the individual single component domains and the combined two-component object.



the Journal of Raman Spectroscopy.11

component adjacency statistics. Domain size statistics were not performed on the blue component due to it being the major component in the formulation and existing as a single large, agglomerated network of particles.

The 3D visualisation demonstrated the association between the API (red) and the green excipient within the tablet matrix. This information could be particularly useful for understanding the stability or dissolution properties of the drug product. By comparing the interactions between components within tablets of the same formulation, which behave differently, we can start to relate how the relative distribution of components within the tablet affect its performance characteristics. By incorporating the component adjacency statistics, we now have a measure of determining the degree of mixing between components within the final tablet. Additionally, accurately obtaining 3D domain number and size statistics for each component can be used to directly compare with the physical properties of the ingoing material and processing parameters used, thus enabling advanced tablet manufacturing understanding.

# **Conclusions**

This paper has summarised the data processing methods required to quantitatively examine 3D vibrational spectroscopic data for pharmaceutical applications and provides a powerful tool for enhanced tablet manufacturing and drug product understanding. The 3D domain size distribution of each component can be determined and used as a comparative tool to understand how the size and shape of domains change throughout the tablet manufacturing process, from raw materials to tablet compaction. Enhanced knowledge regarding the effect of each processing condition on size and shape of the components may lead to optimised manufacturing processes that produce tablets with desired physical and chemical characteristics. The relative position of a component within the drug matrix can also be quantified to assess the spatial arrangement of components within the final drug product. Enhanced understanding regarding the 3D microstructure of a new drug product can provide a baseline understanding of the product with the desired attributes. The spatial arrangement of components within OOS samples can now be quantified and with enhanced process understanding, the root cause may be identified to a single manufacturing step.

# Acknowledgements

This work was supported by Global Technology and Engineering, Pfizer Global Supply.

# Declaration of conflicting interests

The authors declare that they have no conflicts of interest.

## References

- 1. J.A.K. Lauwo, "Effect of particle size and excipients on the dissolution rate of metronidazole from solid dosage forms: II", *Drug Devel. Ind. Pharm.* **10**, 1085 (1984). <a href="https://doi.org/10.3109/03639048409038307">https://doi.org/10.3109/03639048409038307</a>
- A.J. Hlinak, K. Kuriyan, K.R. Morris, G.V. Reklaitis and P.K. Basu, "Understanding critical material properties for solid dosage form design", *J. Pharm. Innov.* 1, 12 (2006). <a href="https://doi.org/10.1007/BF02784876">https://doi.org/10.1007/BF02784876</a>
- 3. F. Kesisoglou and Y. Wu, "Understanding the effect of API properties on bioavailability through absorption modelling", AAPS J. **10**, 516 (2008). <a href="https://doi.org/10.1208/s12248-008-9061-4">https://doi.org/10.1208/s12248-008-9061-4</a>
- 4. J. Gamble, J. Jones and M. Tobyn, "Understanding the effect of API changes in pharmaceutical processing", *Eur. Pharm. Rev.* **22**, 20 (2017).
- A. Kuriyama and Y. Ozaki, "Assessment of active pharmaceutical ingredient particle size in tablets by Raman chemical imaging validated using polystyrene microsphere size standards", AAPS PharmSciTech 15, 375 (2014). <a href="https://doi.org/10.1208/s12249-013-0064-9">https://doi.org/10.1208/s12249-013-0064-9</a>
- 6. H. Carruthers, D. Clark, F. Clarke, K. Faulds and D. Graham, "Comparison of Raman and near-infrared chemical mapping for the analysis of pharmaceutical tablets", *Appl. Spectrosc.* **75**, 178 (2021). <a href="https://doi.org/10.1177/0003702820952440">https://doi.org/10.1177/0003702820952440</a>
- S. Šašić, A. Kong and G. Kaul, "Determining API domain sizes in pharmaceutical tablets and blends upon varying milling conditions by near-infrared chemical imaging", Anal. Meth. 5, 2360 (2013). https://doi.org/10.1039/C3AY26531E
- 8. K.C. Gordon and C.M. McGoverin, "Raman mapping of pharmaceuticals", *Int. J. Pharm.* **417**, 151 (2011). https://doi.org/10.1016/j.ijpharm.2010.12.030

- A.A. Gowen, C.P. O'Donnell, P.J. Cullen and S.E.J. Bell, "Recent applications of chemical imaging to pharmaceutical process monitoring and quality control", Eur. J. Pharm. Biopharm. 69, 10 (2008). https:// doi.org/10.1016/j.ejpb.2007.10.013
- D. Clark and S. Šašić, "Chemical images: technical approaches and issues", Cytometry A: J. Int. Soc. Anal. Cytol. 69, 815 (2006). <a href="https://doi.org/10.1002/cyto.a.20275">https://doi.org/10.1002/cyto.a.20275</a>
- 11. H. Carruthers, D. Clark, F. Clarke, K. Faulds and D. Graham, "Three-dimensional imaging of pharmaceutical tablets using serial sectioning and Raman chemical mapping", *J. Raman Spectrosc.* in press (2022). https://doi.org/10.1002/jrs.6337
- 12. Z. Sun, N. Ya, R.C. Adams and F.S. Fang, "Particle size specifications for solid oral dosage forms: a regulatory perspective", *Amer. Pharm. Rev.* **13**, 68 (2010).
- 13. P. Zarmpi, T. Flanagan, E. Meehan, J. Mann and N. Fotaki, "Biopharmaceutical aspects and implications of excipient variability in drug product performance", *Eur. J. Pharm. Biopharm.* **111**, 1 (2017). https://doi.org/10.1016/j.ejpb.2016.11.004
- 14. N. Charoo, "Critical excipient attributes relevant to solid dosage formulation manufacturing", *J. Pharm. Innov.* **15**, 163 (2019). <a href="https://doi.org/10.1007/s12247-019-09372-w">https://doi.org/10.1007/s12247-019-09372-w</a>
- 15. B.Y. Shekunov, P. Chattopadhyay, H.H.Y. Tong and A.H.L. Chow, "Particle size analysis in pharmaceutics: principles, methods and applications", *Pharm. Res.* **24**, 203 (2007). <a href="https://doi.org/10.1007/s11095-006-9146-7">https://doi.org/10.1007/s11095-006-9146-7</a>
- 16. R. Eyjolfsson, *Design and Manufacture of Pharmaceutical Tablets*. Academic Press (2014).
- 17. D. Clark, M. Henson, F. LaPlant, S. Šašić and L. Zhang, "Pharmaceutical applications of chemical mapping and imaging", in *Applications of Vibrational Spectroscopy in Pharmaceutical Research and Development*, Ed by D.E. Pivonka, J.M. Chalmers and P.R. Griffiths. John Wiley & Sons Ltd, Chichester, UK, p. 309 (2007). <a href="https://doi.org/10.1002/9780470027325.s8913">https://doi.org/10.1002/9780470027325.s8913</a>

- 18. M. Luangtana-Anan and J.T. Fell, "Bonding mechanisms in tabletting", *Int. J. Pharm.* **60**, 197 (1990). https://doi.org/10.1016/0378-5173(90)90073-D
- 19. J. Schindelin, I. Arganda-Carreras, E. Frise, V. Kaynig, M. Longair, T. Pietzsch, S. Preibisch, C. Rueden, S. Saalfeld, B. Schmid, J.-Y. Tinevez, D.J. White, V. Hartenstein, K. Eliceiri, P. Tomancak and A. Cardona, "FIJI: An Open-Source Platform for Biological-Image Analysis", *Nat. Methods* **9**, 676 (2012). https://doi.org/10.1038/nmeth.2019
- 20. C.A. Schneider, W.S. Rasband and K.W. Eliceiri, "NIH Image to ImageJ: 25 years of image analysis", *Nat. Methods* **9**, 671 (2012). <a href="https://doi.org/10.1038/nmeth.2089">https://doi.org/10.1038/nmeth.2089</a>
- 21. J. Schindelin, C.T. Rueden, M.C. Hiner, K.W. Eliceiri, "The ImageJ ecosystem: an open platform for biomedical image analysis", *Mol. Reprod. Dev.* **82**, 518 (2015). https://doi.org/10.1002/mrd.22489
- 22. M. Vidal and J.M. Amigo, "Pre-processing of hyper-spectral images. essential steps before image analysis", *Chemometr. Intell. Lab. Syst.* **117,** 138 (2012). https://doi.org/10.1016/j.chemolab.2012.05.009
- 23. P.Y. Sacré, C. De Bleye, P.F. Chavez, L. Netchacovitch, P. Hubert and E. Ziemons, "Data processing of vibrational chemical imaging for pharmaceutical applications", *J. Pharm. Biomed.* Anal. **101**, 123 (2014). <a href="https://doi.org/10.1016/j.jpba.2014.04.012">https://doi.org/10.1016/j.jpba.2014.04.012</a>
- 24. B. Schmid, J. Schindelin, A. Cardona, M. Longair and M. Heisenberg, "A high-level 3D visualization API for Java and ImageJ", *BMC Bioinform.* **11**, 274 (2010). https://doi.org/10.1186/1471-2105-11-274
- 25. S. Bolte and F.P. Cordelières, "A guided tour into subcellular colocalization analysis in light microscopy", *J. Microsc.* **224**, 213 (2006). <a href="https://doi.org/10.1111/j.1365-2818.2006.01706.x">https://doi.org/10.1111/j.1365-2818.2006.01706.x</a>
- 26. J.F. Gilles, M. Dos Santos, T. Boudier, S. Bolte and N. Heck, "DiAna, an ImageJ tool for object-based 3D co-localization and distance analysis", *Methods* **115**, 55 (2017). <a href="https://doi.org/10.1016/j.ymeth.2016.11.016">https://doi.org/10.1016/j.ymeth.2016.11.016</a>